

Spectral Polarimetric Features Analysis of Wind Turbine Clutter in Weather Radar

Yin, Jiapeng; Krasnov, Oleg; Unal, Christine; Medagli, Stefano; Russchenberg, Herman

DOI

[10.23919/EuCAP.2017.7928348](https://doi.org/10.23919/EuCAP.2017.7928348)

Publication date

2017

Document Version

Accepted author manuscript

Published in

11th European Conference on Antennas and Propagation, EuCap 2017

Citation (APA)

Yin, J., Krasnov, O., Unal, C., Medagli, S., & Russchenberg, H. (2017). Spectral Polarimetric Features Analysis of Wind Turbine Clutter in Weather Radar. In *11th European Conference on Antennas and Propagation, EuCap 2017* (pp. 3351-3355). IEEE. <https://doi.org/10.23919/EuCAP.2017.7928348>

Important note

To cite this publication, please use the final published version (if applicable). Please check the document version above.

Copyright

Other than for strictly personal use, it is not permitted to download, forward or distribute the text or part of it, without the consent of the author(s) and/or copyright holder(s), unless the work is under an open content license such as Creative Commons.

Takedown policy

Please contact us and provide details if you believe this document breaches copyrights. We will remove access to the work immediately and investigate your claim.

Spectral Polarimetric Features Analysis of Wind Turbine Clutter in Weather Radar

Jiapeng Yin, Oleg Krasnov, Christine Unal, Stefano Medagli, Herman Russchenberg
Delft University of Technology, the Netherlands

{ j.yin, o.a.krasnov, c.m.h.unal, s.medagli, h.w.j.russchenberg } @tudelft.nl

Abstract—Wind turbine clutter has gradually become a concern for the radar community for its increasing size and quantity worldwide. Based on the S-band polarimetric Doppler PARSAX radar measurements, this paper demonstrates the micro-Doppler features and spectral-polarimetric characteristic of wind turbine clutter, the probability distribution functions of different spectral-polarimetric variables. Finally, a simple thresholding method to remove wind turbine clutter is put forward, and its effectiveness can be verified by the measured data. This work is expected to contribute to developing effective algorithms for this dynamic clutter suppression for operational weather radar.

I. INTRODUCTION

The high requirement for the renewable energy is expanding over the past several decades. Among these clean energy sources, wind power is the leading source of new power generating capacity in Europe and the United States according to a recent report provided by a global renewable energy policy network. [1]

As more wind turbines are installed, the negative impact of them on different radars, such as ground-based, marine and airborne radars, have been gradually known. In the view of radar, the unwanted echoes from wind turbines, named as wind turbine clutter (WTC), are severe interference that deteriorates the system performance significantly. Normally, one three-bladed wind turbine with a horizontal axis is made up of three main components, the tower, the nacelle and the rotor with blades. The enormous tower and moving blades produce both stationary and non-stationary back-scattering reflection with large intensity. Furthermore, the RCS of the turbine nacelle is a function of its yaw angle, and then, the radar signature will change in agreement with this factor. Echoes from these components may result in high false alarm in the radar detection phase and bias the parameters estimation for further radar application.

The undesirable effect of WTC in weather radar is illustrated in [2] [3]. Methods such as interpolation [4] [5], signal decomposition [6] [7] and machine intelligence technique [8], to mitigate the WTC are investigated by different scholars. It is well recognized that radar polarimetry plays an indispensable role in improving the retrieval of microphysical parameters and in removing non-meteorological scatters. Hence, more research can be done in integrating polarization information into Doppler information. Exploring the Doppler polarimetric property of WTC is the first step as the feature study, which is fundamental for effective WTC mitigation methods proposal. In this paper, we will characterize WTC properties, namely

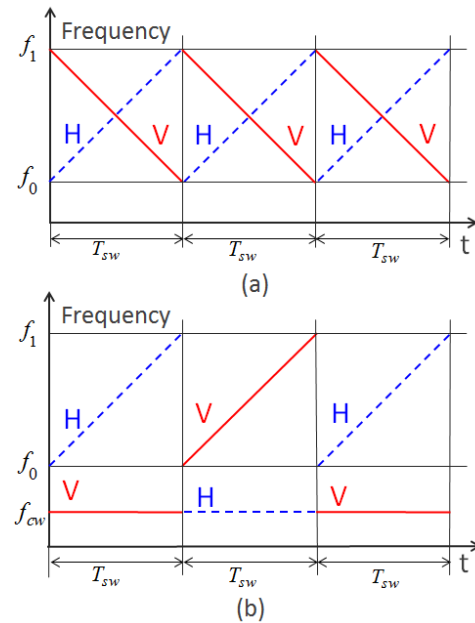


Fig. 1. Polarimetric radar waveforms. (a) LFM signals with dual orthogonality for simultaneous measurements of whole PSM; (b) "Classic" time-multiplexing polarimetric transmit signals for measurements of PSM with two sweeps.

micro-Doppler [9] [10] and spectral-polarimetric. Based on these, a simple WTC removal method, specifically discarding signals whose spectral-polarimetric values are out of the setting thresholds, is proposed and evaluated.

The structure of this paper is as follows. In Section II, the short description of the PARSAX radar system and its configuration for the measurement of polarimetric Doppler characteristics of wind turbine echoes is given together with the concepts of spectral polarimetry. Section III presents the analysis of polarimetric-Doppler properties of observed WTC, the proposed thresholding method of its mitigation, and demonstrates achieved efficiency. Some conclusion and the direction for future study are provided in Section IV.

II. DOPPLER POLARIMETRIC RADAR

A. Radar system

The Delft University of Technology's (TU Delft) PARSAX radar [11] is a high-resolution full-polarimetric S-band Doppler radar. To support the study in exploring the novel

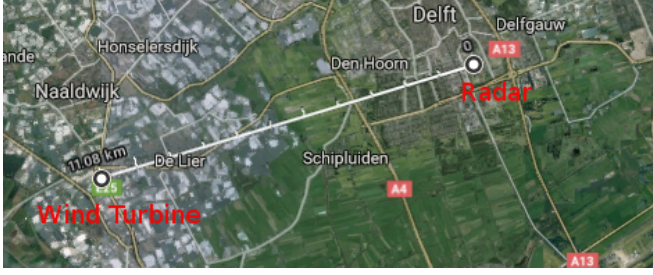


Fig. 2. Google map of the PARSAX radar and the measured wind turbine.

approaches to radar polarimetry, PARSAX was specifically designed to use sounding signals with dual orthogonality for simultaneous measurements of all polarization scattering matrix (PSM) elements. Most of the time, it operates simultaneously transmitting linear-frequency modulated (LFM) signals with up-going frequency excursion via horizontally-polarized port of transmit antenna and with down-going frequency excursion via vertically-polarized port of the same antenna. Both signals occupy precisely the same frequency band (see Fig.1a). Matched processing of signals in two separated channels at the outputs of two parallel polarization receivers provides the possibilities to measure the whole PSM within one sweep.

The software-defined digital architecture of the PARSAX radar up to intermediate frequency provides the capability for real implementation of the waveform agility. This advantage has been used in this study to compare the WTC polarimetric characteristics, which were measured using the simultaneous polarimetry, with "classical" methods when time-multiplexing polarimetric transmit signals are used. In this case, during one sweep the signal with up-going frequency excursion is transmitted via horizontally-polarized port of transmit antenna and two elements of PSM measured in two parallel receiver channels. During the next sweep, the same signal is transmitted via vertically-polarized port of transmit antenna and receivers measure two other elements of PSM. As soon as the power amplifiers of the PARSAX radar could not be blanked on sweep-to-sweep base, agile waveform generator was programmed to generate out of band CW signal in non-operational during current sweep channel (see Fig. 1b).

The sequential, independent records of such polarimetric waveforms scattered by WTC was collected with still antenna system, pointing to one wind turbine around the PARSAX radar location. Fig. 2 displays the scene of the wind turbine measurement campaign. PARSAX radar locates on the roof of the EEMCS faculty building (the position height is about 100 m) on the TU Delft campus while the wind turbine Vestas V66 is 11.08 Km far away from the radar, placed in De Lier, the Netherlands. This type of wind turbine has a 66 m diameter rotor and 78 m tower, as is shown in Fig. 3.

As the linear frequency modulated continuous waveform (LFM-CW) radar, PARSAX was configured to transmit different types of waveforms and the range compression of their received signals has been implemented in real-time within FPGA-based digital receivers. For presented campaign LFM signals with 50 MHz bandwidth have been used that provide final range resolution 3.3 m. For both modes: simultaneously



Fig. 3. The Vestas V66 wind turbine under measurement.

transmitting simultaneously receiving (STSR) H and V polarization, or alternatively transmitting simultaneously receiving (ATSR) dual-polarization, - the same PRF 1 kHz was applied, resulting after Doppler processing of burst with 512 complex range profiles in the Doppler ambiguity $\pm 22.5m/s$ for STSR mode, and $\pm 11.25m/s$ for ATSR mode. The data used for this study can be converted into SNR scale using recorded during the same hour measurements of noise (for such records the mode with blanking of a power amplifier is used).

B. Spectral polarimetry

Based on the combined simultaneous Doppler and polarization information, spectral polarimetry integrates the movement property and microphysical property into a coherent whole. This is favorable to retrieve atmospheric microphysical information and to mitigate non-atmospheric echoes. Following the backscatter alignment (BSA) convention, the spectral reflectivity which relates to the range r and Doppler velocity v is expressed as

$$sZ_{XY}(r, v) = \langle |S_{XY}(r, v)|^2 \rangle \quad (1)$$

where $S_{XY}(r, v)$ represents the complex Doppler velocity spectrum in one range bin with a transmitted Y polarization and a receiving X polarization, X and Y being horizontal or vertical polarization. $\langle \rangle$ represents the time averaging.

Correspondingly, we can define the spectral differential reflectivity sZ_{dr} , spectral linear depolarization ratio $sLDR^{HH}$ and $sLDR^{VV}$, and spectral co-pol correlation coefficient $s\rho_{co}$ as

$$sZ_{dr}(r, v) = 10 \log_{10} \left(\frac{sZ_{HH}(r, v)}{sZ_{VV}(r, v)} \right) \quad (2)$$

$$sLDR^{HH}(r, v) = 10 \log_{10} \left(\frac{sZ_{VH}(r, v)}{sZ_{HH}(r, v)} \right) \quad (3)$$

$$sLDR^{VV}(r, v) = 10 \log_{10} \left(\frac{sZ_{HV}(r, v)}{sZ_{VV}(r, v)} \right)$$

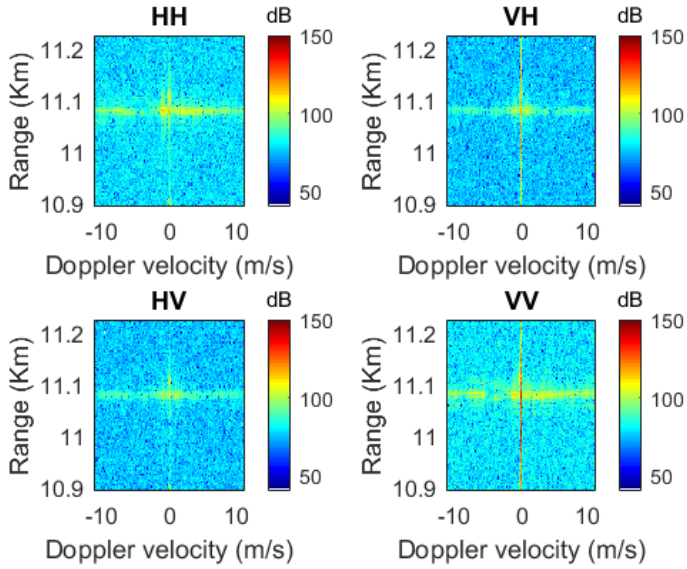


Fig. 4. Range-Doppler spectrogram of wind turbine clutter.

$$s\rho_{co}(r, v) = \frac{\langle S_{VV}(r, v) S_{HH}^*(r, v) \rangle}{\sqrt{\langle |S_{HH}(r, v)|^2 \rangle \langle |S_{VV}(r, v)|^2 \rangle}} \quad (4)$$

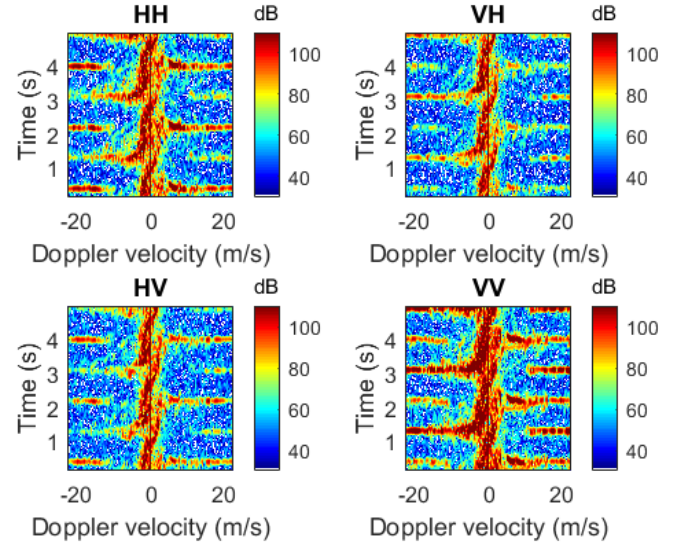
sZ_{dr} is a good indicator of the shape of hydrometeor. Normally, it should be larger than 0 dB for rain. As for $sLDR^{HH}$ and $sLDR^{VV}$, they have been adopted to mitigate clutter for an atmospheric radar slantly or vertically profiling the troposphere. [12] While $s\rho_{co}$ is a very efficient classification variable. $s\rho_{co}$ is very close to 1 for most hydrometeors and significantly lower than 1 for nonmeteorological scatterers measured by the side lobe of the antenna.

Next, all these spectral polarimetric variables will be calculated based on the PARSAX radar measurements, and their statistical distributions will be given.

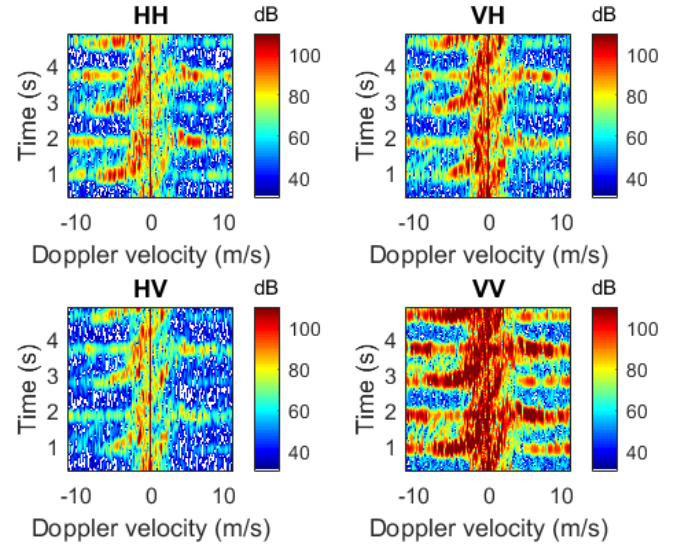
III. MEASUREMENT RESULTS AND ANALYSIS

The measurements took place on July 6th, 2016 in the condition of clear-air and the data were obtained by STSR mode and ATSR mode separately. The azimuth angle and elevation angle were set to 253.85° and -0.15° . For the ATSR mode, the maximum unambiguous Doppler velocity is half of that of STSR mode, because it acquires the full polarimetric information within two sweep times. The operational sweep repetition frequency is 1 KHz and range resolution is 3.3 m. The range-Doppler spectrograms of the four polarization channels of the wind turbine clutter are shown in Fig. 4.

From Fig. 4, we can observe that the wind turbine locates around 11.1 Km (actually it is in the range bin 3357). The reflectivity of wind turbine clutter is so significant that it may lead to false alarm for weather radars. Hence it is essential to mitigate them in operational radars. To have a further check of the micro-Doppler property of WTC, we consider the spotlighted measurement in the range bin 3357 with the time duration of 5 s. Then the Short-Time Fourier Transform



(a)



(b)

Fig. 5. Time-frequency spectrograms of wind turbine clutter measured in two modes: (a) STSR mode; (b) ATSR mode.

(STFT) is applied to both STSR mode and ATSR mode data and the corresponding time-frequency spectrograms are shown in Fig. 5. STFT divides the signal into different sections. The number for the discrete Fourier transform of each section is 256 and the overlapping number between adjoining sections is set to 255 here.

In Fig. 5, the micro-Doppler signature due to the rotation of the blades is presented. Both two modes have the problem of velocity aliasing. However, ATSR suffers more because of the smaller maximum unambiguous Doppler velocity. Also, it is observed that the time period of two neighboring spectrum flash is about 2 s, corresponding to one blade replacing another one in the vertical position. Hence, we can conclude that the rotation period of the three-blade wind turbine is around

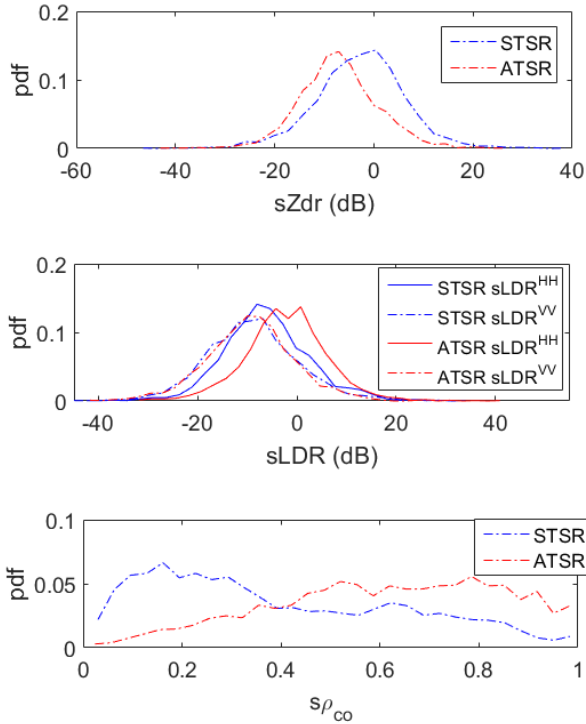


Fig. 6. Experimental pdf of the spectral-polarimetric variables.

6 s. The micro-Doppler property is an obvious indicator of wind turbines, which can provide useful information for WTC detection.

Then based on these measurements, the spectral-polarimetric variables can be calculated, and their probability density functions (pdfs) can be obtained as shown in Fig. 6. The extracted data are in the range bins from 3356 to 3359 as shown in Fig. 4 and all the Doppler bins are included because WTC contains both stationary and non-stationary clutter. From Fig. 6, the sZ_{dr} of WTC is $[-30 \text{ dB}, 20 \text{ dB}]$, and the $sLDR^{HH}$ and $sLDR^{VV}$ are also in the same interval. To be noted, the $s\rho_{co}$ in both modes are widely distributed in $[0, 1]$. This can be an important feature because normally $s\rho_{co}$ is very close to 1 for most hydrometeors, which can be used to mitigate the WTC.

Finally, a simple thresholding method based on these spectral-polarimetric variables is put forward to mitigate the WTC. Combined with the hydrometeors observed by weather radars, the mask $M \in \{0, 1\}$ that characterizes precipitation is expressed as

$$M = \begin{cases} 1, & \text{if } sLDR^{HH} < T_1, sLDR^{VV} < T_1, \\ & T_2 < sZ_{dr} < T_3, s\rho_{co} > T_4 \\ 0, & \text{otherwise} \end{cases} \quad (5)$$

where T_1, T_2, T_3 and T_4 are the set thresholds which can be related in function of the radar configuration and its environment. $M = 1$ represents the potential areas of precipitation.

Here we set $T_1 = -7 \text{ dB}$, $T_2 = -4 \text{ dB}$, $T_3 = 6 \text{ dB}$ and $T_4 = 0.95$. The mask results are shown in Fig. 7. It can be concluded that with such combination almost all the WTC

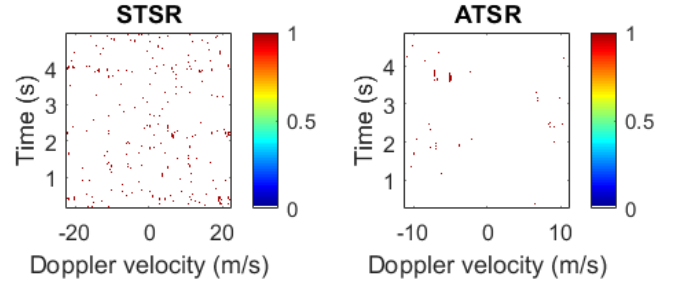


Fig. 7. Results on the thresholding of spectral-polarimetric variables.

are removed, which is favorable. In the future, the pdfs of the spectral-polarimetric variables for the precipitation should also be inspected by conducting another campaign. Then we can design one classifier to distinguish WTC from precipitation.

IV. CONCLUSION

This paper demonstrates the micro-Doppler signature and the spectral-polarimetric properties of wind turbine clutter that were measured using the TU Delft PARSAX radar in two configurations: (a) using dual-orthogonal polarimetric signals for simultaneous measurements of whole polarimetric scattering matrix (simultaneously transmitting simultaneously receiving (STSR) H and V polarization) and (b) using "classic" time-multiplexing polarimetric signals (alternatively transmitting simultaneously receiving (ATSR) H and V polarization). The micro-Doppler signature of WTC was estimated, analyzed and it was demonstrated that it can be used as an important indicator for the WTC detection, while the spectral-polarimetric property can be used to distinguish from weather scatterers. The probability distribution functions of the spectral differential reflectivity, spectral linear depolarization ratio, and spectral co-pol correlation coefficient are given in STSR mode and ATSR mode. Finally, a simple thresholding method to mitigate the WTC signature is proposed, which shows good efficiency with the synthesis of different spectral-polarimetric variables.

The future study should investigate the spectral-polarimetric property of WTC in precipitation. Then with suitable comparison and synthesis, the discriminant to differentiate the precipitation from the WTC should be explored. Additionally, more advanced mitigation should be proposed, not just using simple thresholding. Furthermore, one signal recovery method should also be adopted to deal with the situation when the precipitation and WTC overlap to each other.

V. ACKNOWLEDGMENT

The authors would like to thank Fred van der Zwan and Etienne Goossens for their support in the PARSAX radar maintenance and data collection during the experiment.

REFERENCES

- [1] REN21, "Renewables 2016: global status report," http://www.ren21.net/wp-content/uploads/2016/05/GSR_2016_Full_Report_lowres.pdf, 2016, [Online].

- [2] D. W. Burgess, T. Crum, and R. Vogt, "Impacts of wind farms on WSR-88D radars," in *24th International Conference on Interactive Information and Processing Systems for Meteorology, Oceanography, and Hydrology*, 2008.
- [3] B. Isom, R. Palmer, G. Secrest, R. Rhoton, D. Saxion, T. Allmon, J. Reed, T. Crum, and R. Vogt, "Detailed observations of wind turbine clutter with scanning weather radars," *Journal of Atmospheric and Oceanic Technology*, vol. 26, no. 5, pp. 894–910, 2009.
- [4] F. Kong, Y. Zhang, and R. Palmer, "Wind turbine clutter mitigation for weather radar by adaptive spectrum processing," in *2012 IEEE Radar Conference*. IEEE, 2012, pp. 0471–0474.
- [5] F. Nai, S. Torres, and R. Palmer, "On the mitigation of wind turbine clutter for weather radars using range-Doppler spectral processing," *IET Radar, Sonar & Navigation*, vol. 7, no. 2, pp. 178–190, 2013.
- [6] F. Uysal, I. Selesnick, U. Pillai, and B. Himed, "Dynamic clutter mitigation using sparse optimization," *IEEE Aerospace and Electronic Systems Magazine*, vol. 29, no. 7, pp. 37–49, 2014.
- [7] F. Uysal, I. Selesnick, and B. M. Isom, "Mitigation of wind turbine clutter for weather radar by signal separation," *IEEE Transactions on Geoscience and Remote Sensing*, vol. 54, no. 5, pp. 2925–2934, 2016.
- [8] R. Nepal, J. Cai, and Z. Yan, "Micro-Doppler radar signature identification within wind turbine clutter based on short-cpi airborne radar observations," *IET Radar, Sonar & Navigation*, vol. 9, no. 9, pp. 1268–1275, 2015.
- [9] O. Krasnov and A. Yarovoy, "Polarimetric micro-Doppler characterization of wind turbines," in *2016 10th European Conference on Antennas and Propagation (EuCAP)*. IEEE, 2016, pp. 1–5.
- [10] F. Kong, Y. R. Zhang, and R. Palmer, "Micro-motion signatures of large wind turbines: Case study using a mobile weather radar," in *2016 IEEE Radar Conference (RadarConf)*. IEEE, 2016, pp. 1–4.
- [11] O. A. Krasnov, G. P. Babur, Z. Wang, L. P. Ligthart, and F. Van der Zwan, "Basics and first experiments demonstrating isolation improvements in the agile polarimetric FM-CW radar-PARSAX," *International Journal of Microwave and Wireless Technologies*, vol. 2, no. 3-4, pp. 419–428, 2010.
- [12] C. Unal, "Spectral polarimetric radar clutter suppression to enhance atmospheric echoes," *Journal of atmospheric and oceanic technology*, vol. 26, no. 9, pp. 1781–1797, 2009.